JOURNAL OF APPLIED ELECTROCHEMISTRY **24** (1994) 911–916

Studies on the influence of chloride ion and pH on the electrochemical behaviour of aluminium alloys 8090 and 2014

R. AMBAT, E. S. DWARAKADASA

Department of Metallurgy, Indian Institute of Science, Bangalore - 560 012, India

Received 25 March 1993; revised 22 November 1993

The influence of chloride ion concentration and pH (2.0, 6.0 and 11.0) on the corrosion behaviour of 8090 (Al–Li–Cu–Mg–Zr) and 2014 (Al–4.4%Cu) alloys has been studied in NaCl solution using a potentiodynamic polarization technique. The corrosion rate for both the alloys was high at pH values of 2.0 and 11.0 as compared to that at pH 6.0, and the rate increased in chloride ion concentration at all pH levels. A similar result was found for the passive current density. Increase in pH changed the slope of the cathodic polarization curve by changing the cathodic reaction. Increasing the chloride ion concentration decreased the cathodic reaction rate. On the other hand, the anodic reaction rate increased with increase in chloride ion concentration. The open circuit corrosion potential and the pitting potential shifted in the active (negative) direction with increasing pH and chloride ion concentration. The i_p values for 8090-T851 were slightly lower than those for 2014-T6.

1. Introduction

Aluminium is a reactive metal with a standard electrochemical potential of −1.66 V vs NHE [1]. However, its resistance to corrosion attack is attributed to the presence of a thin, adherent and protective surface oxide film [2]. Protection by this film is limited to environments in which this oxide is only slightly soluble, i.e., between pH 4 to 9 [3]. Above and below this range, aluminium and its alloys normally exhibit uniform attack [3]. Even in solutions in which the oxide film is stable (near neutral pH), the presence of aggressive ions like chloride, creates extensive localized attack [1, 4–7], by adsorption at weak parts of the oxide film and the formation of soluble complexes. The mechanism of pit initiation and growth has been well established, however, the influence of chloride ion is not restricted only to the neutral region (where the oxide film is stable). Direct involvement of anions and cations in metal dissolution reactions in highly acidic and alkaline solutions has been reported by Kolotyrkin [8], Heyrovsky [9], Randles [10], Gerisher [11] and Pointelli [12]. Most of these are on metals like cadmium and mercury. So even in the case of aluminium and its alloys it is presumed that the presence of chloride ion in solution can accelerate the dissolution process at any pH, even though the nature of the attack may differ. Since the primary step i.e. the adsorption of anions at the surface is a competitive process [13, 14], the effect of chloride ion may vary with concentration.

In the present investigation, the influence of chloride ion concentration on the corrosion behaviour of two aluminium alloys namely 8090 (Al–Li–Cu–Mg–Zr) and 2014 (Al–4.4%Cu) have been studied by a potentiodynamic polarization technique at three pH levels namely 2.0, 6.0 and 11.0. These pH levels have been used in view of the fact that they correspond to three regions of the E_h–pH diagram of aluminium. Aluminium–lithium alloy 8090 has been selected for this investigation because of the recent interest in this system due to its light weight and high strength-to-weight ratio which are suitable for structural applications in the aircraft and aerospace industries. Addition of several percent of lithium to these alloys could have a drastic influence on the electrochemical behaviour because of the high reactivity of lithium combined with the precipitation of anodic intermetallic phases $\delta'(Al_3Li)$ and $\delta(AlLi)$. The selection of 2014 is to provide a direct comparison since it is the most used material in the aircraft industry but without any lithium in it.

2. Experimental procedure

For this investigation, 2 mm thick sheets of alloys 8090–T851 (i.e., solutionized at 773 ± 5 K for 2 h, naturally aged, plastically deformed by 1–2% and then stabilized by ageing to peak hardness at 453 ± 1 K for 16–20 h) and 2014-T6 (i.e. solutionized at 773 ± 5 K for 2 h and then peak aged at 453 ± 1 K for 16–20 h) were used. The chemical composition of these alloys is given in Table 1.

Electrochemical polarization measurements were made on 10 mm × 10 mm coupons using an EG & G PARC model 331-3 corrosion measurement system, using a standard three electrode configuration with a saturated calomel reference electrode and a platinum counter electrode. The exposed area of the coupon

Table 1. Chemical composition of the alloys (wt.%)

Element	*8090-T851*	*2014-T6*
Cu	1.2–1.6	4.4
Li	2.5	–
Mg	0.8–1.2	0.5
Fe + Si	0.15	0.8
Zr	0.8–0.12	–
Others	0.15 (max)	0.1 (Mn)

was 1 cm^2. The specimens were first ground on a series of emery papers and then polished on cloth wheels following a conventional metallographic procedure. For 8090 alloy, the lithium depleted layer at the surface (which usually occurs during heat treatment) was removed by continued grinding on emery papers before the experiment. Polarization scans (at a rate of 1 $mV\,s^{-1}$) were carried out in the noble direction after allowing the steady state potential to develop. The experiments were carried out in different concentrations of chloride ions (1–10%) in aerated solutions of different pH. The pH of the solution was adjusted using HCl or NaOH. In all cases duplicate experiments were carried out to ensure reproducibility.

3. Results

3.1. *Influence of pH and chloride ion concentration*

3.1.1. Corrosion rate. Figure 1 shows the plot of corrosion rate vs chloride ion concentration at various pH, calculated using i_{corr} values obtained from polarization curves. At all chloride ion concentrations both the alloys exhibited high corrosion rates at a pH of 2.0 and 11.0, of the order of 20 times that at pH 6.0. The corrosion rate at pH 11.0 is higher than that at pH 2.0. At all pH, corrosion rate increased with increase in chloride ion concentration, but the influence was found to be significant at pH 11.0.

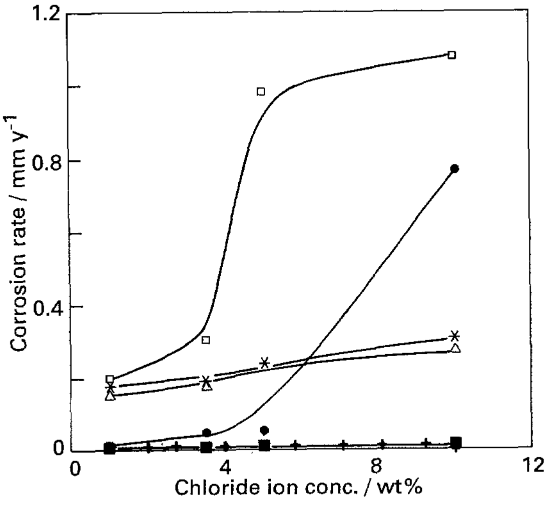

Fig. 1. Dependence of corrosion rate on chloride ion concentration for 8090-T851 ((∗) 2.0, (■) 6.0 (●) 11.0 pH) and 2014-T6 ((△) 2.0, (+) 6.0 and (□) 11.0 pH) in NaCl solution.

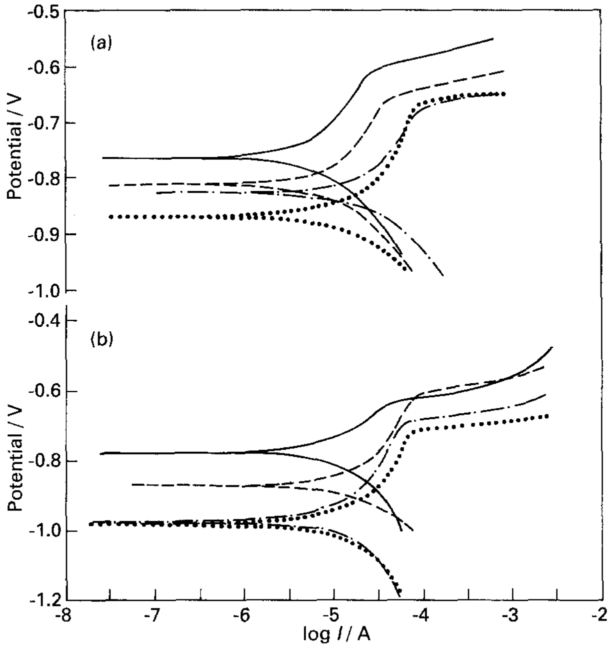

Fig. 2. Potentiodynamic polarization curves for various alloys at pH 2.0 in NaCl solution of different concentrations. (a) 2014-T6 and (b) 8090-T851: (——) 1.0, (– – –) 3.5, (– · –) 5.0 and (· · ·) 10 wt%.

3.1.2. Potentiodynamic polarization. Potentiodynamic polarization curves for both the alloys are shown in Figs. 2, 3 and 4 for pH values of 2.0, 6.0 and 11.0, respectively. Except for 2014 at pH 6.0, all the curves exhibited an apparent active region, with passivity at intermediate values of potential and pitting at and beyond the pitting potential. Both increase in pH and chloride ion concentration shifted the intersecting point of the cathodic and anodic curve (E_{corr}) in the active (negative) direction. Increase in chloride ion concentration shifted the passive region of the anodic curve (except for 2014 at pH 6.0) to higher current density values. The height of the passive region also varied with pH (e.g. for 8090 at pH 2.0 passive region extends for about ∼ 125 mV; corresponding values for 6.0 and 11.0 pH are ∼ 150 and ∼ 600 mV, respectively), but was not affected by increase in chloride ion concentration, except that the value of E_{pp} and E_{pit} shifted to more negative values. Increase in pH of the solution changed the slope of the cathodic curve. Increase in chloride ion concentration decreased the cathodic reaction rate, but the slope of the curve remained almost the same.

Open circuit corrosion potentials (o.c.p.) against chloride ion concentrations at various pH for alloys 8090 and 2014 are given in Fig. 5. The o.c.p. of the aluminium electrode usually depends on the composition of the electrolyte and its pH but is also a function of the period of immersion. As a result, the o.c.p. values were measured after allowing 45 min for development of the steady state potential. The values reported here are averages of the values recorded during the last 10 min. interval. For both the alloys, the o.c.p. is shifted in the negative direction with increase in pH and chloride ion

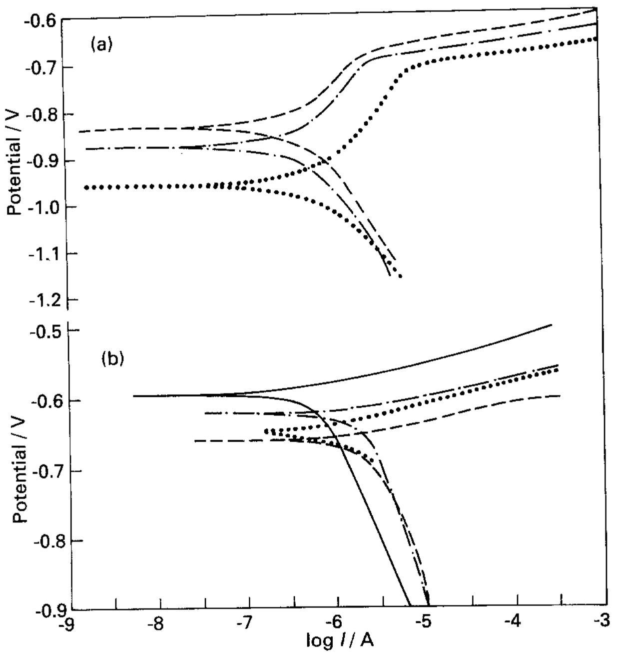

Fig. 3. Potentiodynamic polarization curves for various alloys at pH 6.0 in NaCl solution of different concentrations. (a) 8090-T851 and (b) 2014-T6: (——) 1.0, (– – –) 3.5, (–•–) 5.0 and (• • •) 10 wt %.

concentration, but for pH 2.0 and 11.0 the shift is much slower above 5% NaCl.

Figure 6 gives the plot of passive current density (i_p) against chloride ion concentration for 8090 and 2014. Both alloys showed maximum i_p at pH 2.0. Passivation was not observed for 2014 at pH 6.0. Increase in chloride ion concentration increased the passive current density in all the cases.

Figure 7 shows the plot of pitting potential as a function of chloride ion concentration. The pitting potential is not affected by pH to a great extent, whereas it is shifted in the negative direction with increase in chloride ion concentration in each case, and the magnitude of this shift is almost the same at all pH conditions.

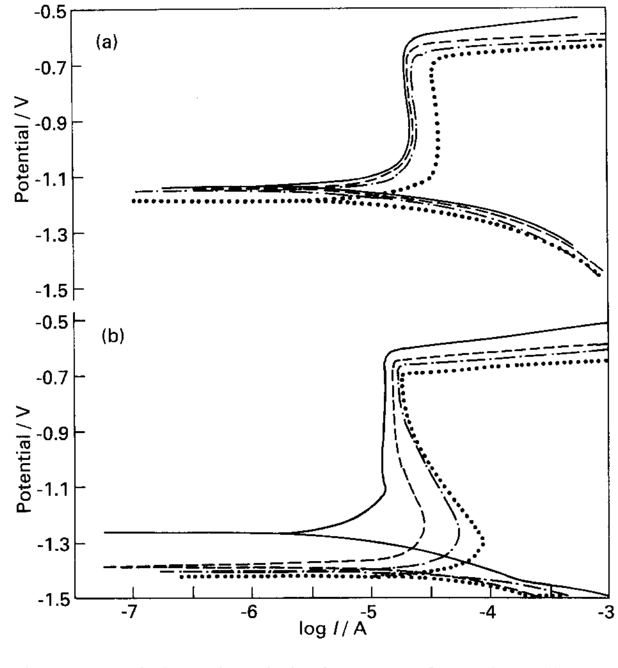

Fig. 4. Potentiodynamic polarization curves for various alloys at pH 11.0 in NaCl solution of different concentrations. (a) 2014-T6 and (b) 8090-T851: (——) 1.0, (– – –) 3.5, (–•–) 5.0 and (• • •) 10 wt %.

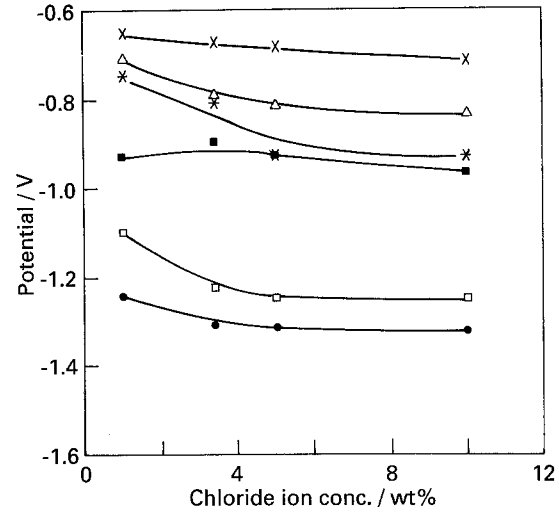

Fig. 5. Dependence of open circuit corrosion potential on chloride ion concentration for 8090-T851 ((∗) 2.0, (■) 6.0 and (●) pH 11.0) and 2014-T6 ((△) 2.0, (×) 6.0 and (□) pH 11.0) alloys.

3.2. *Effect of alloying*

The results given in Figs 1–7 suggest that there is considerable difference in the corrosion and electrochemical behaviour of the two alloys studied (8090 and 2014). These are: (a) 2014 showed higher corrosion rate than 8090 (except at pH 2.0) (Fig. 1), (b) o.c.p. for 2014 is more cathodic (less negative) (Fig. 5), (c) passive current density is higher for 2014 (Fig. 6) and (d) pitting potential is more positive for 2014 (Fig. 7).

4. Discussion

4.1. *Influence of pH*

Solution pH normally influences the corrosion behaviour of aluminium and its alloys by changing the

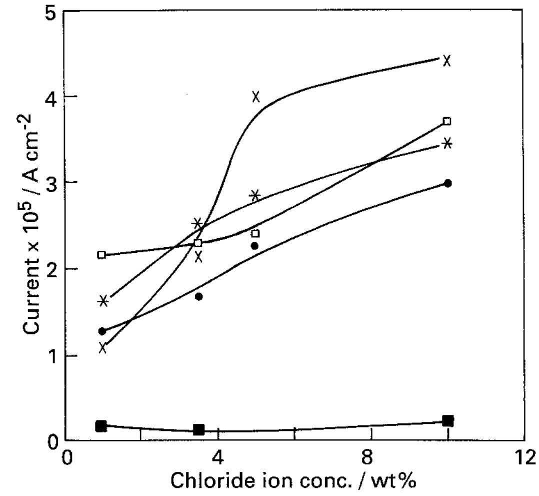

Fig. 6. Dependence of passive current density on chloride ion concentration for 8090-T851 ((∗) 2.0, (■) 6.0 and (●) pH 11.0) and 2014-T6 ((×) 2.0 and (□) pH 11.0) alloys.

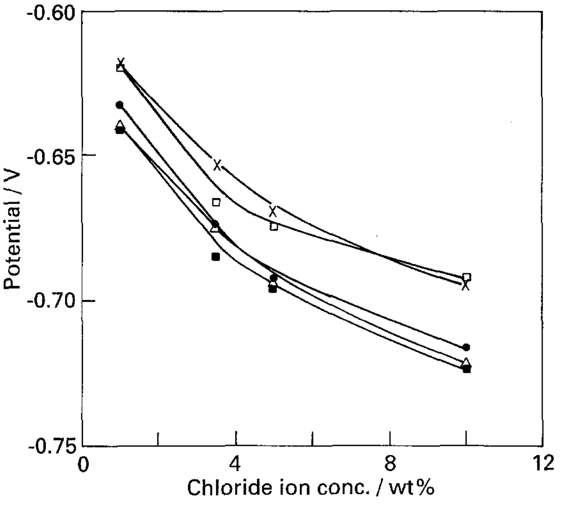

Fig. 7. Dependence of pitting potential on chloride ion concentration for 8090-T851 ((△) 2.0, (■) 6.0 and (●) pH 11.0) and 2014-T6 ((×) 2.0 and (□) pH 11.0) alloys.

stability of the oxide film, as predicted by the Pourbaix diagram [3]. The difference in corrosion rate observed at pH 2.0, 6.0 and 11.0 is then attributed to the change in the stability of the oxide film. In highly acidic and alkaline solutions, the oxide film is highly soluble and this leads to higher corrosion rates of the alloy [3]. Another factor, which enhances corrosion at pH 2.0 is the acceleration of the cathodic reaction, due to the high concentration of H^+ ions. The relatively larger corrosion rates in the alkaline environment is attributed to the highly unstable nature of the Al_2O_3 film in this environment [3].

The dissolution equilibrium in all the three pH conditions is given below.

At pH 2.0, the dissolution equilibrium should be governed by

$$Al = Al^{3+} + 3e^- \qquad (1)$$

In the pH 6.0 condition aluminium is passive and oxygen reduction (if available) will be the primary cathodic reaction. The following reactions represent the dissolution equilibria,

$$Al^{3+} + H_2O = AlOH^{2+} + H^+ \qquad (2)$$

$$Al^{3+} + 2H_2O = Al(OH)_2^+ + 2H^+ \qquad (3)$$

$$Al^{3+} + 3H_2O = Al(OH)_3 + 3H^+ \qquad (4)$$

As the pH increases from acidic, the solubility of Al^{3+} decreases, most likely promoting the precipitation of $Al(OH)_3$.

In the pH 11.0 condition, the dissolution equilibrium is governed by the equation,

$$Al^{3+} + 4H_2O = Al(OH)_4^- + 4H^+ \qquad (5)$$

($Al(OH)_4.2H_2O$ is equivalent to AlO_2^-).

This shows that at pH 2.0 and 11.0, aluminium exists in solution as Al^{3+} and AlO_2^- ions, respectively, where as at pH 6.0, the precipitation of aluminium hydroxide reduces the corrosion rate by protecting the alloy surface.

The intersecting point of the anodic and cathodic curve (E_{corr}) shifted to more negative values with increase in pH as a result of the shift in the cathodic curve as hydrogen ion concentration decreases (equivalent to a change in pH of the solution). The change in slope of the cathodic curve is attributed to the change in the cathodic reaction at different pH levels.

The passive region observed in all the cases (except for 2014 at pH 6.0) is attributed to the formation of a thin oxide film on the surface of the metal, which causes the metal to stop interacting with the surrounding medium [15]. The main factors controlling the formation of this film are the potential of the alloy and the concentration of metallic ion and the interfacial pH. Precipitation of $Al(OH)_3$ occurs when the product of the interfacial OH^- and Al^{3+} ion concentration exceeds the solubility product of $Al(OH)_3$ [15]. The interfacial pH may change due to the reduction of water at these potentials, during cathodic polarization. This is confirmed in the present study, above ~ 1200 mV, by adding small amounts of phenolpthalein, which gives a violet colour near the surface of the specimens due to the production of alkalinity. At pH 2.0, the situation may be different as the interfacial pH shifts from pH 2.0 to a higher value during cathodic polarization and subsequent anodic polarization results in the precipitation of hydroxide, giving rise to passivity. The lower i_p value in the case of pH 6.0 is then attributed to the pH of the solution, which is favourable for the precipitation of $Al(OH)_3$. This is evident in the present study, as maximum passive current density is observed at pH 2.0, where it is very difficult to maintain local alkalinity due to the high acidity of the bulk solution. This type of electrochemical dissolution controlled by surface oxide formation is well known and has been reported by several investigators [15, 16]. A steady state can be attained due to oxide formation/dissolution equilibrium coming into operation.

4.2. *Influence of chloride ion concentration*

The increase in corrosion rate with increase in chloride ion concentration (Fig. 1) is due to the participation of this ion in the metal dissolution reaction. At pH 2.0 and 11.0, the oxide film on the surface is absent; the effect may be due to the direct participation of chloride ion in the metal dissolution reaction. This kind of a mechanism has been predicted by Kolotyrkin and coworkers [8–12] in the case of Cd and Hg. The replacement of water molecules by specifically adsorbed chloride ions at the surface of the dissolving metal increases the overlap of the energy fields which act on the ion from the metallic lattice and the solution, which inevitably facilitates the transfer from the metallic phase to the solution in the form of a complex with adsorbed anions [8]. The reactions can be represented by

$$Me + nA^- \rightarrow (MeA_n)^{n-} \qquad (6)$$

$$(MeA_n)^{n-} \rightarrow (MeA_n)^{(m-n)+} + me^- \qquad (7)$$

Table 2. E^0_{pit} *and* n *values for 8090-T851 and 2014-T6 as function of pH*

pH	*8090-T851*		*2014-T6*	
	E^0_{pit}/V	n	E^0_{pit}/V	n
2.0	−0.711	−0.088	−0.685	−0.080
6.0	−0.715	−0.090	–	–
11.0	−0.710	−0.095	−0.692	−0.090

The first reaction is the specific adsorption which leads to the formation of the complex and the second is the corresponding ionization of the compound.

At pH 6.0, the increase in corrosion rate with increase in chloride ion concentration is attributed to the retardation of the film repair kinetics. The adsorption of chloride ions to weak parts of the oxide film leads to the formation at the film/solution interface of transitional chloride ion containing complexes by the reaction

$$\mathrm{Al} + n\mathrm{Cl}^- \rightarrow \mathrm{AlCl}^{(n-3)-} + 3\mathrm{e}^- \qquad (8)$$

These complexes are much more soluble than the complexes formed in the absence of chloride ions. The dissolution of this complex leads to the breakdown of passivity and hence pitting.

The shift in the o.c.p. towards more negative values (Fig. 5) is attributed to the adsorption of negative chloride ion on the surface of the metal. It has been reported [17] that adsorption of ions on to metal surface changes its potential. The difference in the magnitude of the change in potential with increase in chloride ion concentration for pH 2.0 and 11.0 compared to that for pH 6.0 may be due to the fact that at pH 6.0, the chloride ion adsorption occurs on weak parts of the oxide film, where as for pH 2.0 and 11.0, it occurs directly on the alloy surface.

The reason for the increase in the value of i_p with increase in chloride ion concentration (Fig. 6) is attributed to the stability of the passive film on aluminium and its alloys. The stability of the oxide film depends upon the relative rates of the two reactions, one, the repassivation and the other, the film dissolution [18]. The presence of chloride ions accelerates the latter reaction. This kind of mechanism for the breakdown of passivity in the presence of chloride ions has been reported in the literature [20]. The relative rates of the film-breaking reaction increase with increase in chloride ion concentration and potential, leading to local dissolution (pitting). The onset of pitting is thus the domination of one reaction (attacking effect of chloride ion) over the other (film forming reaction at the base of the flaw). This explains the reason for the increase in i_p values with increase in chloride ion concentration in the present study.

The above mechanism also explains the shift in the pitting potential values towards the active (negative) direction (Fig. 7). The same behaviour has been reported for pure aluminium by M. Yasuda *et al.* [18]. Roth and Kaseche [20] also reported a shift of pitting potential about −0.3 to −0.35 V for 8090-T651 alloy for a change in chloride ion concentration from 0.01 to 1 M.

It has been reported [21] that the chloride ion concentration changes the pitting potential according to the relation:

$$E_p = E^0_p + 2.303n(RT/3F)\log[\mathrm{Cl}^-] \qquad (9)$$

where n represents the stoichiometric factor or reaction order in the pitting reaction. A plot of E_p against $\log[\mathrm{Cl}^-]$ should be linear with a slope of $2.303n(RT/3F)$ and an intercept of E^0_p. The pitting potential values obtained in the present study obeyed the above relationship. The slope and intercept values for both the alloys at different pH are given in Table 2. Both 8090 and 2014 showed almost similar slope values at all pH. The slope corresponding to pH 2.0 is slightly less compared to that of pH 6.0 and 11. Rinker and Duquette [21] found a slope of 106 mV/decade and an intercept of −843 mV for an Al–4.2Mg–2.13Li alloy in NaCl solution. Stirrups *et al.* [22] found a slope of 100 mV/decade and an intercept of −757 mV for pure aluminium and Bohni and Uhlig [23] reported a slope of 124 mV/decade and an intercept of −746 mV for pure aluminium. A comparison of the intercept values for 8090 and 2014 shows that in all pH conditions, lithium-containing alloy 8090 showed more negative values. Thus, for a given electrochemical potential, pits will initiate in the lithium-containing alloys more readily than in 2014.

4.3. *Influence of alloying elements*

The high corrosion rate (Fig. 1) observed for 2014-T6 (except at pH 2.0) may be attributed to the presence of a high percentage of copper, which acts as a probable site for cathodic reaction. Sedricks *et al.* [24] interpreted the faster attainment of steady state pH during *in situ* pH measurements for 7075 compared to that for Al–Zn–Mg alloys by this mechanism. But the low corrosion rate for 8090, which also contains a substantial amount of copper and highly reactive lithium, is not clear. It has been reported for 8090-T851 and 2014-T351 that the presence of dissolved lithium in solution retards the uniform dissolution. More cathodic o.c.p. (less negative) for 2014 is attributed to the presence of a higher amount of copper. It has been reported [25] that copper is one of the elements which can shift the potential of aluminium alloys in the cathodic direction. The lower i_p values obtained for 8090 is due to the stabilization of the oxide film by the incorporation of lithium. There have been several recent investigations [26] which suggest the incorporation of lithium in the oxide film in the case of aluminium alloys. The source of lithium could be either the bulk of the alloy, from which lithium diffuses out, or the solution itself (if it contains lithium ions). A potentiodynamic polarization experiment conducted for pure aluminium in the present study in 0.111 M LiCl and NaCl, shows low i_p values in LiCl solution compared to those in NaCl. Gui and Devine [26] have reported a reduction in passive current density for 6061-T6 in lithium carbonate solution compared to that in sodium carbonate. SIMs analysis of the oxide film showed enrichment of lithium. Roth *et al.* [20] have reported the same kind of behaviour for 8090-T851 alloy and for pure aluminium in sodium sulphate and lithium sulphate solutions. The absence of the passive region in the case of 2014 at pH 6.0 may be explained by the enrichment of copper near the flaws in the oxide film. Yasuda *et al.* [18] have reported the enrichment of copper on the surface in the Al–Cu system. The enrichment of copper on the surface can shift the corrosion potential of the alloy above the pitting potential value. It is well known that when a trace of copper ion is added to a solution of chloride ions, the corrosion potential of aluminium alloys immediately rises nearly as high as the critical pitting potential [27]. According to Bohni and Uhlig [23], the dissolved copper in trace amount deposits on the metal surface and acts as an efficient cathode. But, it has to be mentioned that the 8090 alloy, which also contains a substantial amount of copper, showed passivity at pH 6.0. So the difference may be due to the higher amount of copper in the 2014 alloy.

5. Conclusions

(i) The corrosion rates for 8090 and 2014 alloys in aqueous NaCl solutions are higher at pH 2.0 and 11.0 than at pH 6.0. In all cases increase in chloride ion concentration enhanced the corrosion rate. 2014 alloy showed a higher corrosion rate than 8090.

(ii) Both alloys (except for 2014 at pH 6.0) exhibited passivation in all environments studied. Passive current density increased with increase in pH and chloride ion concentration. O.c.p. showed a shift to more negative (more active) values with increase in pH and chloride ion concentration. Pitting potential also shifted to more negative (more active) values with increase in chloride ion concentration.

(iii) Aluminium–lithium alloy 8090 showed better corrosion resistance than 2014. The passive current density values for 8090 were lower than those for 2014 alloy. However, the pitting potential for 8090 alloy was more negative (more active) than that for 2014.

References

[1] E. Deltombe and M. Pourbaix, *Corrosion* (1958) 496t–500t.
[2] C. Edeleanu and U. R. Evans, *Trans. Faraday. Soc.* **47** (1951) 1121–1135.
[3] M. Pourbaix, 'Atlas of Electrochemical Equilibrium Diagrams in Aqueous Solutions', NACE, Houston, Texas (1966) p. 499.
[4] A. B. McKee and R. H. Brown, *Corrosion* **3** (12) (1947) 595.
[5] W. Beck, F. G. Keihn and R. G. Gold, *J. Electrochem. Soc.* **101** (1954) 393.
[6] Z. Szklarska-Smialowska, 'Pitting Corrosion of Metals', NACE, Houston (1986).
[7] J. R. Galvele, *in* 'Passivity of Metals', (edited by R. Frankenthal and J. Kruger), The Electrochemical Society, Princeton, NJ (1978) p. 285.
[8] J.M. Kolotyrkin, Transactions of the Symposium on Electrode Processes, (edited by Earnest Yeager), pp. 191–196.
[9] J. Heyrovsky, *Discussions Faraday Soc.* **1** (1947) 212.
[10] J. Randles and K. Somerton, *Trans. Faraday Soc.* **48** (1952) 937, 951.
[11] H. Gerischer, *Z. Physik. Chem.* (1953) 202, 292, 302.
[12] R. Pointelli, *Chem. and Ind. (London)* **N40** (1957) 1304.
[13] R. T. Foley, *Corrosion* **42** (1986) 277–288.
[14] K. Videm, Kjeller Report KR-149, Institute for Atommenergi (1974).
[15] L. I. Antropov, *in* 'Theoretical Electrochemistry', Mir Publishers, Moscow (1972) pp. 503–510.
[16] G. A. Dibari and H. J. Read, *Corrosion* **21**(11) (1971) 483.
[17] A. Frumkin, Transactions of the Symposium on Electrode Processes, (edited by Earnest Yeager), pp. 1–15.
[18] M. Yasuda, F. Weinberg and D Tromans, *J. Electrochem. Soc.* **137**, (12) (1990) 3708–3715.
[19] J. Kruger, *in* 'Passivity and its Breakdown on Iron and Iron Base Alloys', USA–Japan Seminar, NACE, Houston, TX (1976) p. 91.
[20] R. Roth and H. Kaseche, *in* Proceedings of the 5th International Aluminium–Lithium Conference, Vol. III (edited by T. H. Sanders, Jr., and E. A. Starke, Jr.), Williamsburg, VA, 27–31 March (1989) p. 1207.
[21] R. E. Rinker and D. J. Duquette, 'Aluminium–Lithium Alloys II', TMS–AIME, Warrendale, PA (1984) p. 581.
[22] B. N. Stirrup, N. A. Hampson and I. S. Misgley, *J. Appl. Electrochem.* **5** (1975) 229.
[23] H. Bohni and H. H. Uhlig, *J. Electrochem. Soc.* **116**, (7) (1969) 906.
[24] A. J. Sedricks, J. A. J. Green and D. L. Novak, *Corrosion* **27** (1971) 199.
[25] M. Reboul and P. Meyer, *in* Proceedings of the 4th International Aluminium–Lithium Conference, Vol. II, (edited by G. Champier, B. Dubost, D. Mianny and L. Sabetay), France, 10–12 June (1987) p. C-3-881.
[26] J. Gui and T. M. Devine, *Scri. Met.* **21** (1987) 853.
[27] S. Furuya and N. Soga, *Corrosion* **46** (1990) 989–993.